ADVANCED FUNCTIONAL MATERIALS

FULL PAPER

DOI: 10.1002/adfm.200700355

Highly Efficient Non-Doped Blue-Light-Emitting Diodes Based on an Anthrancene Derivative End-Capped with Tetraphenylethylene Groups**

By *Ping-I Shih*, *Chu-Ying Chuang*, *Chen-Han Chien*, *Eric Wei-Guang Diau*, and *Ching-Fong Shu**

A novel blue-emitting material, 2-*tert*-butyl-9,10-bis[4-(1,2,2-triphenylvinyl)phenyl]anthracene (**TPVAn**), which contains an anthracene core and two tetraphenylethylene end-capped groups, has been synthesized and characterized. Owing to the presence of its sterically congested terminal groups, **TPVAn** possesses a high glass transition temperature (155 °C) and is morphologically stable. Organic light-emitting diodes (OLEDs) utilizing **TPVAn** as the emitter exhibit bright saturated-blue emissions (Commission Internationale de L'Eclairage (CIE) chromaticity coordinates of $x = 0.14$ and $y = 0.12$) with efficiencies as high as 5.3 % (5.3 cd A^{-1})—the best performance of non-doped deep blue-emitting OLEDs reported to date. In addition, **TPVAn** doped with an orange fluorophore served as an authentic host for the construction of a white-light-emitting device that displayed promising electroluminescent characteristics: the maximum external quantum efficiency reached 4.9 % (13.1 cd A^{-1}) with CIE coordinates located at (0.33, 0.39).

1. Introduction

Organic light-emitting devices (OLEDs) have been attracting considerable attention because of their potential application within flat-panel displays.[1,2] Efficient blue-light OLEDs are of particular interest because they are desired for use as blue light sources in full-color display applications;[3–8] furthermore, they can also serve as hosts for exothermic energy transfer to lower-energy fluorophores to realize white-light OLEDs.[9–13] Although the use of dopant emitters in the guest-host system can improve the electroluminescence (EL) efficiency significantly,[14–16] the addition of dopants is usually a complicated and expensive process during the mass production of OLEDs. Because phase separation upon heating is an important cause of performance degradation in some guest (or dopant)-host systems[17–19] and considering that some of these OLEDs will be operated under harsh conditions (, e.g., at high temperatures), the use of a single-component host emitting layer may be more pragmatic for application than the use of guest-host-type emitting layers. Although several blue host emitters have been reported for the fabrication of non-doped blue OLEDs,[4–8,20,21] high-performance blue-light-emitting materials exhibiting ideal color purity, good stability, and high fluorescence efficiency remain relatively rare.

Because anthracene derivatives possess outstanding photoluminescence and electroluminescence properties, they have been used widely as emitting materials in OLEDs.[12,15,22–25] In this paper, we report the synthesis and characterization of a novel, deep-blue-emitting material, 2-*tert*-butyl-9,10-bis[4-(1,2,2-triphenylvinyl)phenyl]anthracene (**TPVAn**, Scheme 1), for use in non-doped blue-light OLEDs. In **TPVAn**, two tetraphenylethylene groups are end-capped at the 9- and 10-positions of the central anthracene core to increase structural bulk and non-planarity through the tendency of the phenyl rings to twist. The non-planarity of this molecular structure effectively diminishes its degree of intermolecular π–π stacking and reduces concentration quenching; meanwhile, the sterically bulky units facilitate the formation of stable amorphous films.[25,26] In addition, we expected that the introduction of a *tert*-butyl unit

Scheme 1. Synthetic Pathway of TPVAn

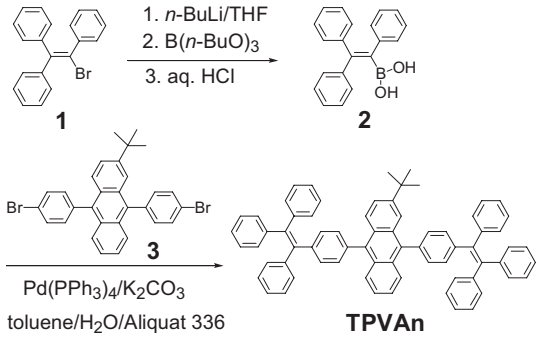

Scheme 1. Synthetic pathway of TPVAn

[*] Prof. C.-F. Shu, P.-I. Shih, C.-Y. Chuang, C.-H. Chien, Prof. E. W.-G. Diau
Department of Applied Chemistry, National Chiao Tung University
Hsinchu, 300 (Taiwan ROC)
E-mail: shu@cc.nctu.edu.tw

[**] We thank the National Science Council for financial support. Our special thanks go to Professor C.-H. Cheng for his support and cooperation during the preparation and characterization of the light-emitting devices.

at the C2 position of the anthracene moiety might enhance the morphological stability of this material's thin films during annealing processes.[25,27] In comparison with other blue-light-emitting materials for non-doped OLEDs, **TPVAn** provides higher thermal stability, good color purity, and better emitting efficiency.

2. Results and Discussion

2.1. Synthesis

Scheme 1 illustrates the synthetic route used for the preparation of the anthracene derivative end-capped with two tetraphenylethylene moieties. The lithiation of commercially available 1-bromo-1,2,2-triphenylethene (**1**) with an excess of *n*-BuLi, followed by treatment with *n*-butyl borate and hydrolysis in aqueous HCl, gave 1,2,2-triphenylvinylboronic acid (**2**). The key intermediate, 2-*tert*-butyl-9,10-bis(4-bromophenyl)anthracene (**3**), was obtained as reported previously by reaction of monolithiated 1,4-dibromobenzene with 2-*tert*-butylanthraquinone and then reduction of the intermediate diol with potassium iodide and sodium hypophosphite in acetic acid.[25] Subsequent Pd-catalyzed Suzuki coupling between the boronic acid **2** and the dibromide **3** afforded the target compound. The structure of **TPVAn** was characterized using ^{1}H and ^{13}C NMR spectroscopy, elemental analysis, and high-resolution mass spectrometry.

2.2. Thermal Properties

The thermal properties of **TPVAn** were investigated through thermogravimetric analysis (TGA) and differential scanning calorimetry (DSC). **TPVAn** exhibits high thermochemical stability, as evidenced (through TGA) by a 5 %-weight-loss temperature under nitrogen atmosphere of 445 °C (inset of Fig. 1). DSC was performed in the temperature range from 40 to 330 °C. Figure 1 displays the DSC curves of a sublimated sample of **TPVAn**, which melted at 298 °C on the first heating only, and then changed into a glassy state upon cooling from the melt. When the amorphous glassy sample was heated again, a glass transition occurred at 155 °C; no exothermic peak due to crystallization appeared at temperatures up to 350 °C. On subsequent cooling and heating cycles, only the glass transition phenomenon remained in the DSC thermogram, i.e., without recrystallization. The prominent stability of the amorphous glass state of **TPVAn** is due presumably to the presence of the sterically bulky tetraphenylvinyl end-capping groups coupled with the rigid *tert*-butyl-substituted anthracene core. In addition, the high molecular weight of **TPVAn** may also play a role in raising its glass transition temperature.

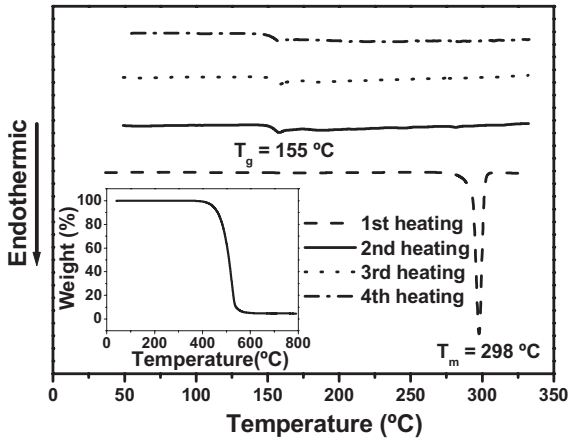

Figure 1. DSC traces of TPVAn recorded at a heating rate of 20 °C min^{-1}. Inset: TGA thermogram of TPVAn recorded at a heating rate of 20 °C min^{-1}.

Because of its excellent thermal and morphological stabilities, we were able to prepare homogeneous and stable amorphous thin films of **TPVAn** through vacuum deposition. As revealed by atomic force microscopy (AFM), an evaporated film of **TPVAn** exhibited (Fig. 2) a uniform surface that underwent no morphological changes when annealed at 100 °C for 9 h under a nitrogen atmosphere; the root-mean-square surface roughness of this annealed film was very narrow (0.33 nm). In contrast, annealing a film of 9,10-di(2-naphthyl)anthracene (**ADN**), which is a prototypical material for blue-light-emitting electroluminescent devices,[28,29] induced the degradation of the surface morphology and the formation of large crystals on the annealed layer.[30] Thus, our thermal analysis of **TPVAn** clearly demonstrates that it possesses excellent thermal stability and is a potent blue-light-emitting material that inhibits crystallization in the solid state.

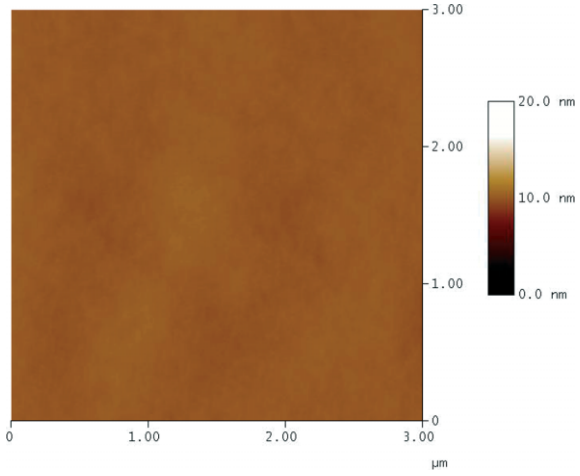

Figure 2. AFM topographic image (tapping mode) of a TPVAn film after annealing at 100 °C for 9 h under a nitrogen atmosphere. The film was vapor-deposited onto a silicon wafer under vacuum.

2.3. Photophysical Properties

Figure 3 displays the absorption and photoluminescence (PL) spectra of **TPVAn** in dilute solution and as a solid film on a quartz plate. For the sample in THF solution, we attribute the absorption peaks in the region from 350 to 400 nm with

ADVANCED FUNCTIONAL MATERIALS

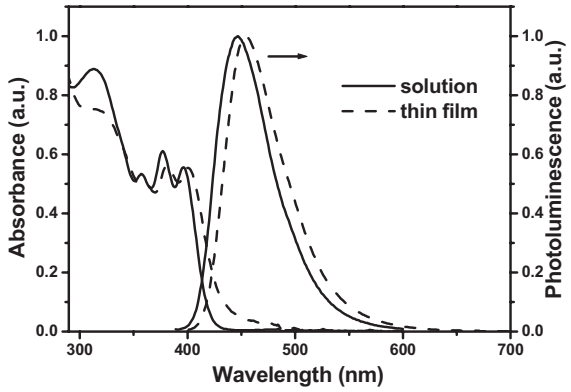

Figure 3. UV-vis absorption and PL spectra of TPVAn in dilute THF solution (solid lines) and in the solid state (dashed lines).

characteristic vibronic pattern to the π–π* transitions of anthracene,[31] and the absorption band at 316 nm to the π–π* transitions of the peripheral 4-(1,2,2-triphenylvinyl)phenyl groups.[32] Upon excitation at 380 nm, the solution displays a blue PL having an emission maximum at 448 nm. The absorption and emission spectra of the **TPVAn** thin film are similar to those obtained in dilute solution, but with red-shifts of 3 and 6 nm, respectively. These small spectral shifts in the solid state spectra suggest that if any intermolecular interactions occurred they were quite weak, i.e., they were restrained effectively by the bulky tetraphenylvinyl groups. Although **TPVAn** exhibited a weak blue emission in solution, e.g., its fluorescence quantum yield in cyclohexane was 0.06 [using 9,10-diphenylanthracene ($\Phi_f = 0.90$) as the reference], the blue emission was greatly enhanced in the solid state. In addition, when we blended **TPVAn** with poly(methyl methacrylate) (PMMA), the resultant film emitted a bright blue light; the quantum yield of 0.89 [relative to 9,10-diphenylanthracene (1.0)] was significantly higher than the value measured in solution. We attribute this enhanced emission to the restricted intramolecular rotation of the phenyl peripheries in the solid state.[33–35] In dilute solution, twisting of the olefinic double bond of the 4-(1,2,2-triphenylvinyl)phenyl group might facilitate approach between the excited and ground states of **TPVAn** and, thus, the occurrence of efficient internal conversion; this situation is similar to tetraphenylethylene undergoing rapid radiationless decay along the ethylenic torsional coordinate.[36,37] In the solid state, however, the degree of internal conversion was insignificant because the rigid environment inhibited the twisting motion of **TPVAn,** resulting in the observed enhanced emission.

2.4. Electroluminescence Properties of LED Devices

To evaluate the applicability of using **TPVAn** as the emitting layer (EML), we fabricated three different non-doped blue-emitting devices (I–III, Fig. 4) through sequential vapor deposition of the materials onto ITO glass under vacuum (3×10^{-6} Torr); the fabrication and characterization of these EL devices are similar to techniques we have reported previously.[38] Device I was designed as our standard blue-light-emitting device having the following configuration: indium tin oxide (ITO)/4,4′-bis[*N*-(1-naphthyl)-*N*-phenylamino] biphenyl (NPB) (30 nm)/(**TPVAn**) (40 nm)/ 1,3,5-tris(*N*-phenylbenzimidazol-2-yl)benzene (TPBI) (40 nm)/ Mg:Ag (100 nm)/Ag (100 nm). NPB and TPBI were employed as the hole-transporting layer (HTL) and the electron-transporting layer (ETL), respectively. Figure 5 and Table 1 summarize the EL characteristics of device I. Using the conventional NPB as the HTL, the device exhibited a maximum external quantum efficiency of 3.1 % (3.1 cd A^{-1}) at 17.6 mA cm^{-2} with Commission Internationale de L'Eclairage (CIE) color coordinates located at (0.15, 0.11); these values reveal that the emitter **TPVAn** possesses an authentic and promising blue emission. For comparison and optimization purposes, in device II we replaced NPB with a novel fluorene/triarylamine hybrid, tris[4-(9-phenylfluoren-9-yl)phenyl]amine (TFTPA), which possesses a larger ionization potential (IP), a larger energy gap, and a smaller electron affinity (EA) relative to those of NPB.[39] Device II displayed enhanced EL performance in comparison with device I; its maximum external quantum efficiency reached 4.1 % (4.1 cd A^{-1}) at 25.8 mA cm^{-2} (see Fig. 5 and Table 1). According to the energy level diagram

Table 1. Performance of Devices I–IV.

Device	I	II	III	IV
Turn-on voltage [V] [a]	3.9	3.4	4.9	3.9
Voltage [V] [b]	6.6	6.2	6.7	9.3
Brightness (cd/m^2)[b,c]	625 (2961)	810 (3614)	993 (4165)	2234 (9125)
E.Q.E. [%] [b,c]	3.1 (3.0)	4.1 (3.6)	5.0 (4.2)	4.2 (3.4)
L.E. [cd/A] [b,c]	3.1 (3.0)	4.0 (3.6)	5.0 (4.2)	11.2 (9.1)
Max E.Q.E. [%]	3.1	4.1	5.3	4.9
Max L.E. [cd/A]	3.1	4.1	5.3	13.1
Max P.E. [lm/W]	1.5	2.1	2.8	7.5
EL λ_{max} [nm] [d]	454	454	456	556
CIE, *x* and *y*[d]	0.15 and 0.11	0.14 and 0.11	0.14 and 0.12	0.33 and 0.39

[a] Recorded at 1 cd m^{-2}. [b] Recorded at 20 mA/cm^2. [c] Data in parentheses were recorded at 100 mA/cm^2. [d] At 7 V.

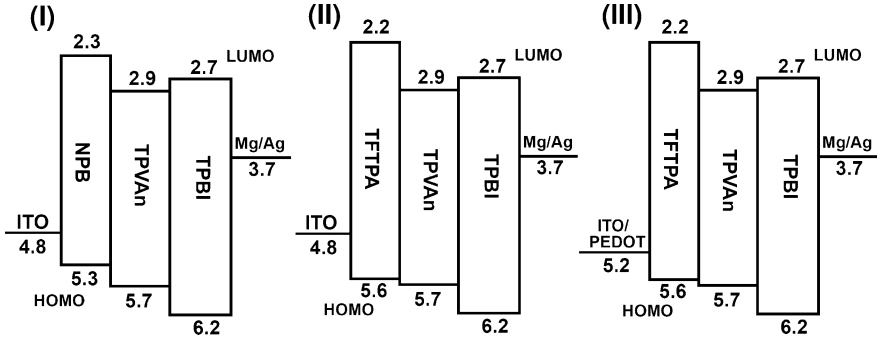

Figure 4. Energy level diagrams for the OLED devices I–III.

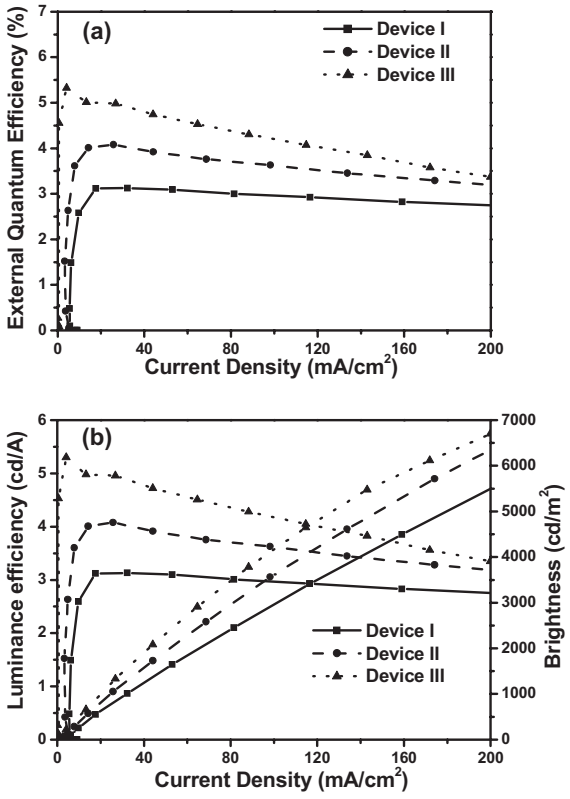

Figure 5. Plots of a) external quantum efficiency and b) luminance efficiency and brightness as functions of the current density for devices I-III.

based deep-blue-light-emitting OLEDs (Table 2).[16,43] Moreover, in devices I-III the high EL efficiency occurred at the brightness of ca.. 1000 cd m^{-2}, which appears to be more practical for commercial applications; even at a high current density (ca. 100 mA cm^{-2}), these three devices displayed gratifying levels of efficiency (e.g., 4.2 % and 4.2 cd A^{-1} for device III).

According to the EL spectra in Figure 6, devices I–III all exhibited saturated deep blue emissions with peak maxima centered at 454 nm that did not shift upon changing the applied voltage. These EL spectra were quite similar to the PL spectrum of the **TPVAn** film, indicating that both the EL and PL originated from the same radiative decay process of singlet excitons and that all of the emissions originated exclusively from the **TPVAn** layer in these devices, with no emission interference from adjacent carrier transporting layers. Figure 6 and Table 1 indicate that the corresponding CIE coordinates of devices I-III were very close to the standard blue emission recommended by the National Television Standards Committee (NTSC).

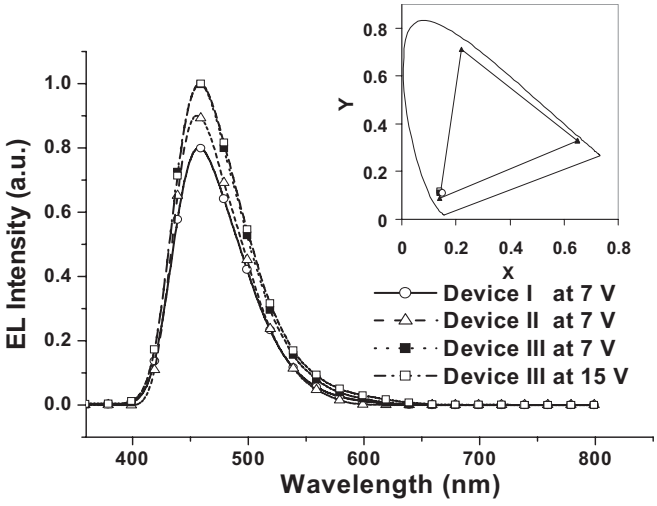

Figure 6. EL spectra of devices I–III at an applied voltage of 7 V, and of device III at an applied voltage of 15 V. Inset: Respective CIE coordinates.

in Figure 4, we attribute this improved device efficiency to the smaller barrier for hole injection from the HTL to the EML and to the better electron-blocking capability of TFTPA (EA = 2.2 eV) relative to that of NPB (EA = 2.3 eV). As a result, more excitons can be confined within the emissive layer. We note that device II exhibited lower driving voltages than did device I. This finding implies that the operating voltages also would be influenced by the energy offset between the HOMO energy levels of the HTL and the EML, which is smaller in device II. Similar observations have been reported.[40,41] In device III, we inserted a well-known hole injection material poly(styrenesulfonate)-doped poly(3,4-ethylenedioxythiophene) (PEDOT) between the ITO anode and TFTPA (HTL) to smoothen the relatively rough ITO layer, reduce the interfacial surface area, and lower the leakage current.[42] The insertion of a PEDOT layer in device III led to slightly higher driving voltages, due to the increase of the total thickness of organic layers.[42] Nevertheless, this subtle adjustment had a significant impact on the device efficiency; indeed, device III exhibited the highest efficiency among these three devices: its maximum external quantum efficiency of 5.3 % (5.3 cd A^{-1}) at 4.1 mA cm^{-2} is the highest reported to date for any non-doped deep-blue-light-emitting OLED, and is comparable to those of guest-host-

In addition to the non-doped deep-blue OLEDs, we also fabricated a white-light-emitting device (device IV), using **TPVAn** as the host material, having the following architecture: ITO/PEDOT/NPB (30 nm)/**TPVAn**:0.25 wt % of 4-(dicyanomethylene)-2-*tert*-butyl-6-(1,1,7,7-tetramethyljulolidyl-9-enyl)-4*H*-py-

Table 2. Electroluminescence data for the deep-blue-light-emitting OLEDs (na: not available).

Device architecture	Emitting material	Max E.Q.E. [%]	Max L.E. [cd/A]	Emission wavelength	CIE (*x*, *y*)	Ref.
Non-doped	Anthracene derivative	5.3	5.3	456	(0.14, 0.12)	This paper
Non-doped	Distyrylbenzene derivative	na	4.8	460	(0.16, 0.13)	[4]
Non-doped	2,2′-Bistriphenylenyl	4.2	4.0	458	(0.14, 0.11)	[5]
Non-doped	Spirobifluorene derivative	4.2	3.6	450	(0.15, 0.09)	[6]
Doped	Styrylamine derivative	5.1	5.4	na	(0.14, 0.13)	[16]

ADVANCED FUNCTIONAL MATERIALS

ran (DCJTB) (40 nm)/TPBI (30 nm)/Mg:Ag (100 nm)/Ag (100 nm). The EL spectrum of device IV (Fig. 7) displays a composite emission band: one signal (at ca. 456 nm) is a characteristic emission of the **TPVAn** host, while the other (at

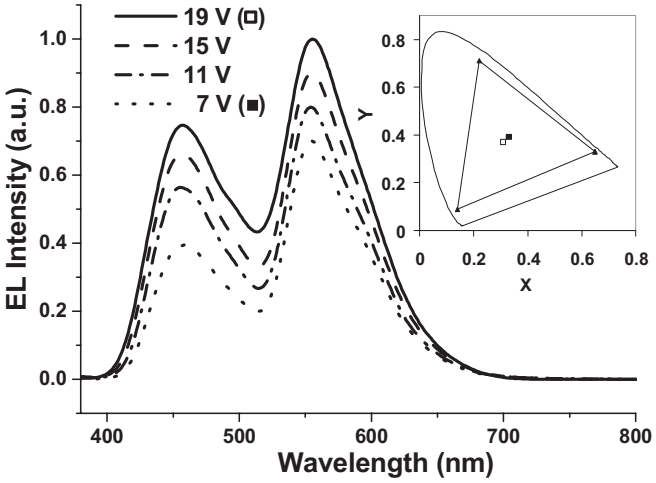

Figure 7. EL spectra of device IV operated at various driving potentials. Inset: Respective CIE coordinates.

ca. 556 nm) originates from the emission of DCJTB. The corresponding CIE coordinates of this white-light-emitting device were located at (0.33, 0.39), close to the central region of white light. Furthermore, the CIE coordinates of device IV underwent a negligible shift from (0.33, 0.39) at 7 V to (0.31, 0.37) at 19 V (inset of Fig. 7), reflecting its insensitivity toward changes in the operating potential. Moreover, this device exhibited a satisfying EL performance (Fig. 8): the maximum luminance was above 30 000 cd m^{-2} at 19 V and the maximum external quantum efficiency reached as high as 4.9 % (13.1 cd A^{-1}), which is superior to that of other conventional fluorescent white-light-emitting OLEDs.[9,10,12,13] In addition, when we increased the luminance of our white-light-emitting device up to the order of 5×10^3 cd m^{-2} (at ca. 52 mA cm^{-2}), the corresponding EL efficiency remained above 10 cd A^{-1}.

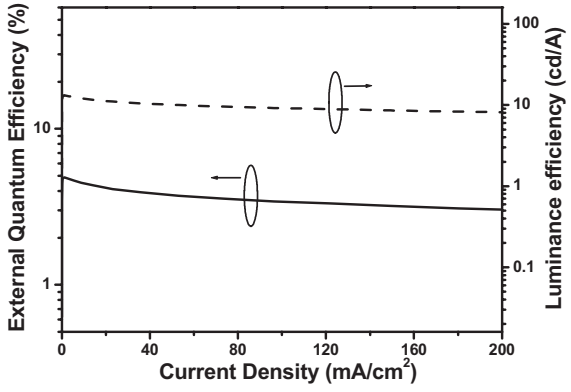

Figure 8. External quantum efficiency and luminance efficiency plotted as functions of the current density for device IV.

3. Conclusions

We have realized efficient deep-blue non-doped OLEDs based on a novel highly thermally stable blue-light-emitting material, **TPVAn**, which comprises a 2-*tert*-butylanthracene core and two sterically bulky tetraphenylethylene peripheral groups. The **TPVAn**-based non-doped devices exhibited satisfying deep-blue emissions with CIE coordinates located at ca. (0.14, 0.11), very close to the standard blue CIE coordinates. Moreover, these devices displayed excellent EL efficiency: the maximum external quantum efficiency reached 5.3 % (5.3 cd A^{-1}) at 4.09 mA cm^{-2}—the best performance reported to date for non-doped deep-blue-light-emitting OLEDs. In addition to achieving highly efficient blue fluorescence, we demonstrated that **TPVAn** doped with an orange fluorophore could serve as an authentic host for the construction of a white-light-emitting device that displayed promising EL characteristics: CIE coordinates located at (0.33, 0.39) and maximum external quantum efficiency reaching 4.9 % (13.1 cd A^{-1}).

4. Experimental

Characterization: ^{1}H and ^{13}C NMR spectra were recorded using Varian UNITY INOVA 500 MHz, Varian Unity 300 MHz, and Bruker-DRX 300 MHz spectrometers. Mass spectra were obtained using a JEOL JMS-HX 110 mass spectrometer. DSC analysis was performed using a SEIKO EXSTAR 6000DSC unit operated at heating and cooling rates of 20 and 50 °C min^{-1}, respectively. Samples were scanned from 40 to 330 °C, cooled to 0 °C, and then scanned again from 40 to 330 °C. The glass transition temperatures (T_g) were determined from the second heating scan. Thermogravimetric analysis was undertaken using a DuPont TGA 2950 instrument. The thermal stabilities of the samples under a nitrogen atmosphere were determined by measuring their weight loss while heating at a rate of 20 °C min^{-1}. UV-vis spectra were measured using an HP 8453 diode-array spectrophotometer. PL spectra were obtained using a Hitachi F-4500 luminescence spectrometer. The HOMO energies of organic thin films were measured using a Riken-Keili AC-2 atmospheric low-energy photoelectron spectrometer; the LUMO energies of materials were estimated by subtracting the optical energy gap from the measured HOMO. Atomic force microscopy measurements were performed using a Digital Nanoscope IIIa in tapping mode under ambient conditions.

1,2,2-Triphenylvinylboronic Acid (***2***): *n*-Butyllithium in hexane (6.0 mL, 2.5 M) was added slowly under nitrogen to a stirred solution of 1-bromo-1,2,2-triphenylethene (**1**, 2.00 g, 5.99 mmol) in anhydrous THF (40 mL) at –78 °C. Gradually, the color of the reaction mixture changed to green; the stirring was continued for 30 min, while the temperature was raised to –20 °C. The reaction mixture was cooled to –78 °C and then tri-*n*-butylborate (4.05 mL, 15.0 mmol) was added dropwise. This mixture was warmed to room temperature and stirred for another 8 h. Thereafter, the reaction mixture was quenched with aqueous HCl (2.0 M, 10 mL) and extracted with diethyl ether (2 × 25 mL). The combined organic phases were dried ($MgSO_4$) and concentrated under reduced pressure. The crude product was washed several times with *n*-hexane to give **2** (1.50 g, 83.5 %). ^{1}H NMR (300 MHz, $CDCl_3$): δ 4.13 (s, 2H), 6.88–6.92 (m, 2H), 7.00–7.19 (m, 8H), 7.29–7.38 (m, 5H). ^{13}C NMR (75 MHz, $CDCl_3$): δ 126.2, 127.0, 127.6, 128.2, 128.4, 128.6, 129.3, 129.8, 130.7, 141.9, 142.2, 143.7, 153.2. MS (*m*/*z*): 300 $[M]^+$.

2-tert-Butyl-9,10-bis(4-(1,2,2-triphenylvinyl)phenyl)anthracene (***TPVAn***): Aqueous K_2CO_3 (2.0 M, 10 mL) was added to a solution of **2** (1.35 g, 4.50 mmol), 2-*tert*-butyl-9,10-bis(4-bromophenyl)anthracene (**3**, 1.00 g,

1.84 mmol), and Aliquat 336 (ca. 220 mg) in toluene (30 mL). After degassing, tetrakis(triphenylphosphine)palladium (ca. 25 mg) was added under a flow of nitrogen, and then the mixture was heated at 110 °C while stirring under nitrogen. After 5 h, the reaction mixture was cooled to room temperature and then poured into aq. methanol (70 % methanol, 80 mL); the yellow precipitate was filtered off, washed with methanol, and dried under vacuum. This crude product was purified through column chromatography (*n*-hexane/EtOAc, 9:1) to afford **TPVAn** (1.10 g, 67.2 %) as a yellowish powder. ^{1}H NMR (300 MHz, $CDCl_3$): δ 1.30 (s, 9H), 7.08–7.22 (m, 37H), 7.26–7.33 (m, 3H), 7.43 (dd, J = 9.2, 2.0 Hz, 1H), 7.56–7.62 (m, 4H). ^{13}C NMR (125 MHz, $CDCl_3$): δ 30.9, 35.0, 121.2, 124.36, 124.45, 124.7, 126.52, 126.56, 126.8, 126.9, 127.6, 127.7, 127.8, 128.3, 129.4, 129.7, 129.9, 130.6, 130.8, 131.2, 131.28, 131.37, 131.41, 131.5, 136.4, 136.6, 137.10, 137.16, 140.9, 141.0, 141.2, 141.5, 142.9, 143.0, 143.4, 143.5, 143.7, 143.8, 143.9, 147.0. HRMS (*m*/*z*): [M^+ + H] calcd. for $C_{70}H_{55}$ 895.4304; found 895.4299. Anal. Calcd for $C_{70}H_{54}$: C, 93.92; H, 6.08. Found: C, 94.06; H, 6.22.

Received: March 27, 2007
Revised: June 6, 2007
Published online: September 20, 2007

[1] T. Fuhrmann, J. Salbeck, *MRS Bull.* **2003**, *28*, 354.
[2] C. W. Tang, S. A. Van Slyke, *Appl. Phys. Lett.* **1987**, *51*, 913.
[3] C. Hosokawa, *Synth. Met.* **1997**, *91*, 3.
[4] Y. Duan, Y. Zhao, P. Chen, J. Li, S. Y. Liu, F. He, Y. G. Ma, *Appl. Phys. Lett.* **2006**, *88*, 263 503.
[5] H. T. Shih, C. H. Lin, H. H. Shih, C. H. Cheng, *Adv. Mater.* **2002**, *14*, 1409.
[6] J. Y. Shen, C. Y. Lee, T. H. Huang, J. T. Lin, Y. T. Tao, C. H. Chien, C. T. Tsai, *J. Mater. Chem.* **2005**, *15*, 2455.
[7] C. C. Wu, Y. T. Lin, K. T. Wong, R. T. Chen, Y. Y. Chien, *Adv. Mater.* **2004**, *16*, 61.
[8] R. C. Chiechi, R. J. Tseng, F. Marchioni, Y. Yang, F. Wudl, *Adv. Mater.* **2006**, *18*, 325.
[9] J. H. Jou, Y. S. Chiu, R. Y. Wang, H. C. Hu, C. P. Wang, H. W. Lin, *Org. Electron.* **2006**, *7*, 8.
[10] C. H. Chuen, Y. T. Tao, F. I. Wu, C. F. Shu, *Appl. Phys. Lett.* **2004**, *85*, 4609.
[11] J. Kido, H. Shionoya, K. Nagai, *Appl. Phys. Lett.* **1995**, *67*, 2281.
[12] T. H. Liu, Y. S. Wu, M. T. Lee, H. H. Chen, C. H. Liao, C. H. Chen, *Appl. Phys. Lett.* **2004**, *85*, 4304.
[13] Y. S. Wu, S. W. Hwang, H. H. Chen, M. T. Lee, W. J. Shen, C. H. Chen, *Thin Solid Films* **2005**, *488*, 265.
[14] C. W. Tang, S. A. Van Slyke, C. H. Chen, *J. Appl. Phys.* **1989**, *65*, 3610.
[15] M. T. Lee, H. H. Chen, C. H. Liao, C. H. Tsai, C. H. Chen, *Appl. Phys. Lett.* **2004**, *85*, 3301.
[16] M. T. Lee, C. H. Liao, C. H. Tsai, C. H. Chen, *Adv. Mater*. **2005**, *17*, 2493.
[17] G. Y. Zhong, Z. Xu, S. T. Zhang, W. Huang, X. Y. Hou, *Appl. Phys. Lett.* **2002**, *81*, 1122.
[18] S. C. Chang, G. He, F. C. Chen, T. F. Guo, Y. Yang, *Appl. Phys. Lett.* **2001**, *79*, 2088.
[19] J. R. Gong, L. J. Wan, S. B. Lei, C. L. Bai, X. H. Zhang, S. T. Lee, *J. Phys. Chem. B* **2005**, *109*, 1675.
[20] S. L. Tao, Z. K. Peng, X. H. Zhang, P. F. Wang, C. S. Lee, S. T. Lee, *Adv. Funct. Mater.* **2005**, *15*, 1716.
[21] F. I. Wu, C. F. Shu, T. T. Wang, E. W. G. Diau, C. H. Chien, C. H. Chuen, Y. T. Tao, *Synth. Met.* **2005**, *151*, 285.
[22] Y. H. Kim, D. C. Shin, S. H. Kim, C. H. Ko, H. S. Yu, Y. S. Chae, S. K. Kwon, *Adv. Mater.* **2001**, *13*, 1690.
[23] Y. H. Kim, H. C. Jeong, S. H. Kim, K. Yang, S. K. Kwon, *Adv. Funct. Mater.* **2005**, *15*, 1799.
[24] W. J. Shen, R. Dodda, C. C. Wu, F. L. Wu, T. H. Liu, H. H. Chen, C. H. Chen, C. F. Shu, *Chem. Mater.* **2004**, *16*, 930.
[25] K. Danel, T. H. Huang, J. T. Lin, Y. T. Tao, C. H. Chuen, *Chem. Mater.* **2002**, *14*, 3860.
[26] S. Wang, W. J. Oldham, Jr., R. A. Hudack, Jr., G. C. Bazan, *J. Am. Chem. Soc.* **2000**, *122*, 5695.
[27] J. Shi, *Eur. Patent 1156 536*, **2001**.
[28] Y. Li, M. K. Fung, Z. Xie, S. T. Lee, L. S. Hung, J. Shi, *Adv. Mater.* **2002**, *14*, 1317.
[29] J. Shi, C. W. Tang, *Appl. Phys. Lett.* **2002**, *80*, 3201.
[30] S. W. Wen, M. T. Lee, C. H. Chen, *J. Display Technol.* **2005**, *1*, 90.
[31] *Handbook of Fluorescence Spectra of Aromatic Molecules*, 2nd ed. (Ed: I. B. Berlman), Academic, New York, **1971**.
[32] C. E. Bunker, N. B. Hamilton, Y. P. Sun, *Anal. Chem.* **1993**, *65*, 3460.
[33] N. J. Turro, *Modern Molecular Photochemistry*, University Science Books, Sausalito, CA **1991**.
[34] J. Luo, Z. Xie, J. W. Y. Lam, L. Cheng, H. Chen, C. Qiu, H. S. Kwok, X. Zhan, Y. Liu, D. Zhu, B. Z. Tang, *Chem. Commun.* **2001**, 1740.
[35] Q. Zeng, Z. Li, Y. Dong, C. Di, A. Qin, Y. Hong, L. Ji, Z. Zhu, C. K. W. Jim, G. Yu, Q. Li, Z. Li, Y. Liu, J. Qin, B. Z. Tang, *Chem. Commun.* **2007**, 70.
[36] P. F. Barbara, S. D. Rand, P. M. Rentzepis, *J. Am. Chem. Soc.* **1981**, *103*, 2156.
[37] E. Lenderink, K. Duppen, D. A. Wiersma, *J. Phys. Chem.* **1995**, *99*, 8972.
[38] F. I. Wu, P. I. Shih, M. C. Yuan, A. K. Dixit, C. F. Shu, Z. M. Chung, E. W. G. Diau, *J. Mater. Chem.* **2005**, *15*, 4753.
[39] F. I. Wu, P. I. Shih, C. H. Chien, A. K. Dixit, C. F. Shu, submitted.
[40] C. Q. Ma, L. Q. Zhang, J. H. Zhou, X. S. Wang, B. W. Zhang, Y. Cao, P. Bugnon, M. Schaer, F. Nüesch, D. Q. Zhang, Y. Qiu, *J. Mater. Chem.* **2002**, *12*, 3481.
[41] D. E. Loy, B. E. Koene, M. E. Thompson, *Adv. Funct. Mater.* **2002**, *12*, 245.
[42] E. L. Williams, K. Haavisto, J. Li, G. E. Jabbour, *Adv. Mater.* **2007**, *19*, 197.
[43] M. H. Ho, Y. S. Wu, S. W. Wen, M. T. Lee, T. M. Chen, C. H. Chen, K. C. Kwok, S. K. So, K. T. Yeung, Y. K. Cheng, Z. Q. Gao, *Appl. Phys. Lett.* **2006**, *89*, 252 903.